Nanoplasmon Coupled Intracellular Optical Resonance Excitation for Ultrasensitive 3D Fluorescence Cell Imaging

Manas Ranjan Gartia[1,5], Austin Hsiao[2,5], Mayandi Sivaguru[3], Yi Chen[4,5], G. Logan Liu[2,4,5,*]
[1]Department of Nuclear, Plasma and Radiological Engineering, University of Illinois
[2]Department of Bioengineering, University of Illinois
[3]Institute for Genomic Biology, University of Illinois
[4]Department of Electrical and Computer Engineering, University of Illinois
[5]Micro and Nanotechnology Laboratory, University of Illinois, Urbana 61801, USA
*Correspondence should be addressed to G.L.L. (loganliu@illinois.edu)

ABSTRACT

We have created an enhanced cell-imaging platform for 3D confocal fluorescence cell imaging where fluorescence sensitivity is amplified for more than 100 folds especially for cell membrane and cytoplasm. The observed unprecedented three-dimensional fluorescence intensity enhancement on the entire cell microstructure including cell membrane 10 μm above the substrate surface is attributed to a novel far field enhancement mechanism, nanoplasmon coupled optical resonance excitation (CORE) mechanism which permits enhanced surface plasmon on the substrate being evanescently coupled to Whispering Gallery mode optical resonance inside the spheroidal cell membrane microcavity. Theoretical model of the hypothesis is explained using coupled mode theory. In addition, preliminary result has been provided for the observation of early stage of transfection in a cancer cell.

Keywords: Confocal microscopy, surface plasmon, cell imaging, metal enhanced fluorescence

1. INTRODUCTION

Fluorescence cell imaging technique is one of the most powerful and ubiquitous methods in cell biology research due to its specificity and high sensitivity[1]. Besides the instrumentation, the limitations to the fluorescence cell imaging sensitivity include the quantum yield and photostability of fluorophore as well as the auto-fluorescence of the cells. Recently a new strategy has been deployed to increase the fluorescence signal from the organic dyes using metal coated slides for cell imaging which mainly rely on the principle of smooth or nanostructured metal enhanced fluorescence [2-5]. The enhancement of fluorescence signal near a smooth metal surface (approximately a factor of 4~5) is due to the mirror reflection of both excitation light and fluorescence emission[2]. Whereas the fluorescence enhancement near a nanostructured noble metal surface is due to surface plasmon resonance facilitated electromagnetic field enhancement in near field[6]. The nanostructured metal enhanced fluorescence is highly distance dependent and the surface plasmon coupled emission extends only up to tens of nanometer above the metal surface[7]. With a sharp contrast here we demonstrate a fundamentally new scientific mechanism for far-field fluorescence enhancement by creating extremely strong intracellular optical resonance modes.

Optical resonance is a concept commonly used in laser device in which a pair of mirror surfaces forms a standing wave cavity resonator for light waves. Light confined in the cavity reflects multiple times with little attenuation producing strong standing waves at certain resonance frequencies. The standing wave patterns produced are called modes. Additional optical resonances include guided-mode resonances[8] in a waveguide and surface plasmon resonance with high evanescent fields at a dielectric-metallic interface. A circular or spherical dielectric structure can also serve as the cavity or waveguide to support optical resonance modes, in this case, called whispering gallery modes (WGM). In the WGM optical resonance, every photon guided by the total internal reflection is forced to recirculate many times within circular dielectric cavity, thereby increasing the intensity of the effective optical field built up inside[9, 10]. If one can create WGM optical resonance modes guided by the spheroidal cell membrane microstructure, the effective intracellular light excitation field can be enhanced dramatically even for a few orders of magnitude for a high-Q resonator. Now the key

Biosensing and Nanomedicine IV, edited by Hooman Mohseni, Massoud H. Agahi, Manijeh Razeghi,
Proc. of SPIE Vol. 8099, 80990T · © 2011 SPIE · CCC code: 0277-786X/11/$18 · doi: 10.1117/12.893128

Downloaded From: http://proceedings.spiedigitallibrary.org/ on 04/22/2017 Terms of Use: http://spiedigitallibrary.org/ss/termsofuse.aspx

question is: how to couple the laser excitation into the intracellular whispering gallery optical resonance mode in a 3D confocal fluorescence microscopy imaging system?

We designed and manufactured a unique nanoplasmonic device to couple laser light into intracellular WGM optical resonance for intensified fluorescence excitation. Surface plasmon polaritons are optically induced electron oscillation at the interface between metal and dielectric materials when wave vector matching requirements at the metal-dielectric interface is fulfilled. Additionally surface plasmon polaritons may be enhanced by metallic nanostructures[11]. Under proper configuration, the nanostructure enhanced surface plasmon excited by incident laser light wave can be coupled to the surface-bounded whispering gallery mode optical resonance in a spherical dielectric cavity, e.g. a spheroidal cell in water or air, which results in highly amplified optical excitation and enhanced fluorescence emission on cell membrane and nearby cytoplasm. Although it has not been demonstrated previously, the far field coupling of light into whispering gallery mode (WGM) optical resonance in a living cell has been postulated[10]. The feasibility of surface plasmon polaritons coupling to whispering gallery microdisk resonators and micropillar resonators have been demonstrated both experimentally and theoretically[12, 13].

Based on the completely new nanoplasmon CORE mechanism, we demonstrate a highly amplified (more than 100 folds maximum enhancement with respect to the case of a glass slide substrate) three-dimensional fluorescence cell imaging facilitated by a novel silver nanopillar plasmonic substrate. As proposed above, the whispering gallery mode (WGM) optical resonance excitation on the spheroidal cell membrane cavity waveguide is created and evanescently coupled by the resonant plasmon polaritons which are enhanced on the metal coated nanopillar substrate where the cell situates.

2. MATERIALS AND METHODS

2.1 Nanoplasmonic device fabrication

The nanocone structures are fabricated by photolithography and reactive ion etching process. In order to make high-aspect-ratio nanocone structures, an etching-passivation method is used. First, the native oxide layer is removed from the poly crystal silicon wafer using a wet etch process (buffered oxide etching). Then the required micro area arrays (dot arrays) in to which nanopillar structures are to be etched are patterned by photolithography. Secondly, by using a mixture of HBr and O2 gases, the polysilicon substrate is etched by HBr and oxidized by O_2 simultaneously. In few seconds a nano-mask made of silicon oxybromide natually forms, and then HBr gas is further used to etch uncovered polysilicon substrate. Since, HBr has a high etching selectivity of polysilicon to oxide (200: 1), high-aspect-ratio nanocone structures can be created. Finally, to render it with plasmonic property a thin layer of (80 nm) silver coating is provided on the top of the nanopillar structure using E-beam evaporation.

2.2 Cell culture

The Chinese Hamster Ovary (CHO) cells are maintained in Ham's F12 medium containing 5% fetal bovine serum (FBS), 1% antibioticantimycotic solution (10 units/mL penicillin G sodium, 10 ug/mL streptomycin sulfate, 25 ug/mL amphotericin B, 0.85% saline; Invitrogen, Carlsbad, CA), and 1% glutamine and grown in 100 mm glass culture plates at 37 °C in a humidified atmosphere of 5% CO2. The cells exhibit normal morphology, express cell contact inhibition and grow as a monolayer without expression of neoplastic foci. CHO cells are transferred when the culture becomes confluent. For the experiment, the cells are re-suspended to 1e6 cells per mL. For the confocal imaging, the cells are seeded on the nanopillar plasmonic structure and incubated at 37 °C in a humidified atmosphere of 5% CO2 for at least 12 hours to allow attachment.

2.3 Cell labeling procedure

FM 1-43 FX (Cat # F35355, Invitrogen) dye is used to stain the cell membrane. A working staining solution of 5 ul/ml dye in ice-cold PBS solution is prepared. The ice-cold temperature is followed as the dyes are quickly endocytosed. Finally, the nanoplasmonic substrate with the cells is washed with fresh PBS before immersing in the staining solution for about one minute. The substrate is immediately taken for the imaging.

Fluo-4, AM (Cat # F23917, Invitrogen) dye is used to monitor the calcium (Ca+2) level of the cell (stain for the cytoplasm), but used here as a label for the viable cell cytoplasm. A working staining solution of 5 ul/ml dye in fresh PBS solution is prepared. The substrate with cells on top of it is washed with fresh media and then immerse in the staining solution. The substrate with the cells is incubated with the staining solution for 15 minutes at 37 °C in a humidified atmosphere of 5% CO2 before imaging.

Downloaded From: http://proceedings.spiedigitallibrary.org/ on 04/22/2017 Terms of Use: http://spiedigitallibrary.org/ss/termsofuse.aspx

The cell nucleus is stained with blue fluorescent Hoechst dyes (Invitrogen, Hoechst 33342, trihydrochloride, trihydrate; Cat # H3570). The substrate with the cells is incubated in a 2 ul/ml staining solution for about 15 minutes at 37 °C and a humidified atmosphere of 5% CO2 before imaging.

2.4 Confocal imaging

The cell imaging is performed by Zeiss LSM 710 Confocal Microscope. The microscope system consists of a Zeiss 710 confocal scanner, Axio Observer Z1 microscope and a Spectraphysics Mai-Tai Ti-Sapphire laser. Out of the available seven visible excitation lines (405nm, 458nm, 488nm, 514nm, 561nm, 594nm, 633nm), three are used for our experiment (405 nm, 488 nm and 561 nm). The microscope is equipped with QUASAR 34 channel spectral detector (2 standard PMTs and a 32 channel PMT array) with spectral resolutions up to 3 nm. ZEN 2009 software is used for the hardware control and spectral un-mixing. The laser power used for the experiment is about 0.2% of the total available power (25 mW).

2.5 SEM fixation procedure

The cell media is replaced by fixative (2.0 % paraformaldehyde and 2.5% glutaraldehyde (both E.M. grade) in 0.1 M Na-Cacodylate buffer, pH 7.4) and kept for 4 hours in a 4 oC refrigerator. Then the cells are rinsed with buffer solution (0.1 M Na-Cacodylate buffer, pH 7.4) for 10 minutes on a shaker table. After the buffer rinse, graded dehydration (37% ethanol, 10 min; 67% ethanol, 10 min; 95% ethanol, 10 min; 100% ethanol, 3 x 10 min) is performed for the cells. Finally, all the ethanol in the sample is replaced by carbon dioxide by performing critical point drying (CPD) in a 100% ethanol environment. Prior to SEM imaging the sample was sputter-coated with 7-nm Gold-palladium coating and the imaging is performed using Philips XL30 ESEM-FEG in Hi-Vac mode.

3. RESULTS AND DISCUSSION

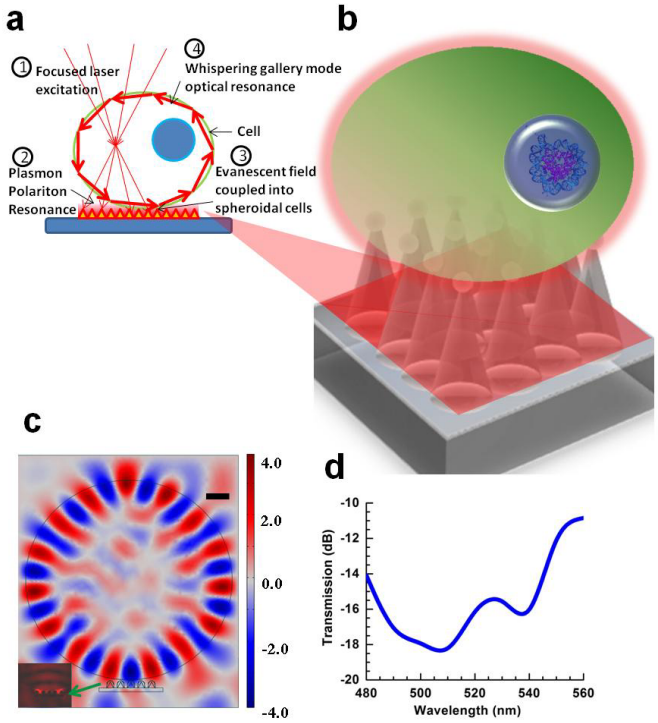

Figure 1. Mechanism of nanoplasmon coupled whispering gallery mode optical resonance in cell (a) The schematic of the experimental set up (b) The schematic of the device showing the plasmonic structure and a cell on the structure. (c) Simulation of whispering gallery mode of a spherical cell on the nanopillar plasmonic structure in transverse electric (TE) mode using finite element method. (d) Transmittance near WGM

Downloaded From: http://proceedings.spiedigitallibrary.org/ on 04/22/2017 Terms of Use: http://spiedigitallibrary.org/ss/termsofuse.aspx

In our experimental configuration (Fig. 1a) living cells are situated on top of a nanoplasmonic substrate which is composed of tightly packed silicon nanocone array covered by a thin layer of silver. The silver coated nanocone array as depicted in Fig. 1b can support both propagating surface plasmon and localized plasmon at visible wavelength range. Additionally the silver coated nanocone structures are capable of "nano-focusing" or "concentrating" optical energy creating high electromagnetic field[14] which can then be coupled to a cell. Our two-dimensional finite element analysis supports the Nanoplasmon CORE mechanism for the proposed three-dimensional far field fluorescence enhancement. The transverse electric field of a WGM optical resonance is shown in Fig. 1c . The inset shows the electromagnetic field enhancement due to nanocone array plasmonic structure. For this particular geometry of the spherical cell with the diameter of 2 μm, WGM optical resonance occurs at 559 THz (536 nm). The possibility of surface plasmon coupling to WGM optical resonance has been confirmed using other plasmonic structures and cell dimensions.

In our experiments, Chinese hamster ovary (CHO) cells[15, 16] are grown on the nanoplasmonic substrate. The cell membrane and nucleic acid of the live cell are stained with fluorescent dyes respectively in one set of experiments. In another sets of experiments fluorescent labels are applied to calcium ions in the cytoplasm and the chromosome in nuclei respectively. The labeled CHO cells on the nanoplasmonic structure are imaged via high-resolution laser scanning confocal microscopy. The 405 nm, 488 nm and 561 spectral lines were used for the excitation of respective fluorophore dyes. As shown in Fig. 1a, the laser beam is illuminated on the nanoplasmonic substrate after focusing through the cell. Plasmon polaritons are optically excited in the nanocone array structure, then coupled back again into the cell through the physical contact interface and converted into the propagating WGM optical wave. To confirming the cell attachment and growth on the nanoplasmonic substrate, a scanning electron micrograph of the tapered silicon nanocone before and after coated with an 80 nm thick silver layer is shown in Fig. 2a & b. Spherical and spheroidal CHO cells sitting and spreading on the nanopillar surface are imaged through the scanning electron microscope and shown in Fig. 2c & d.

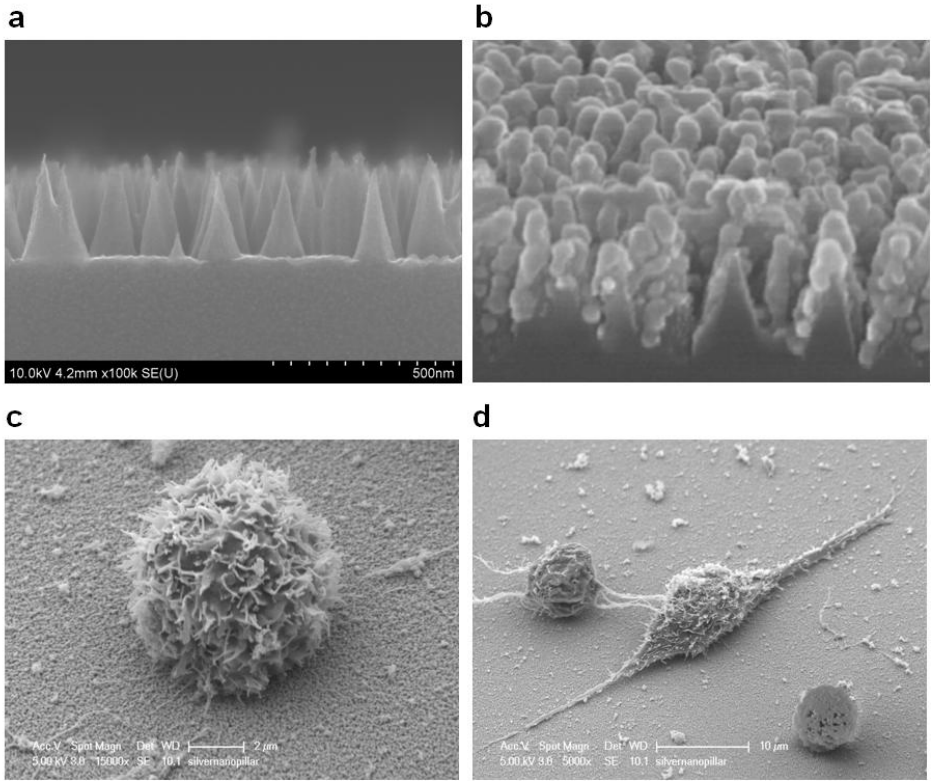

Figure 2. SEM of nanoplasmonic structure (a) before Ag deposition (b) after 80 nm Ag deposition and CHO cells cultured on it (c) spheriodal CHO cell (d) elongated CHO cell.

A typical bright field image of large number of cells grown on the substrate is shown in Fig. 3a. For the comparison purpose, we intentionally patterned the substrate surface to make an array of square areas with silver nanopillar

Downloaded From: http://proceedings.spiedigitallibrary.org/ on 04/22/2017 Terms of Use: http://spiedigitallibrary.org/ss/termsofuse.aspx

plasmonic structure and the rest of substrate surface is covered with a smooth silver film. Due to the far field fluorescence enhancement facilitated by Nanoplasmon CORE technology, only the cytoplasm calcium (label in green fluorescence) in the cell grown on the nanoplasmonic substrate can be observed in 3D fluorescence imaging (Fig. 3b) with an extremely low laser power and short imaging time (0.2% of 25 mW laser power for green fluorescence excitation and 1.58 μs pixel dwell time) while other cells on smooth silver surface exhibit undetectable to extremely low fluorescence emission only except near the immediate surface of smooth silver film. It should be noted that the fluorescence intensity below and beyond cell span is due to the point spread function of the fluorescence emission.

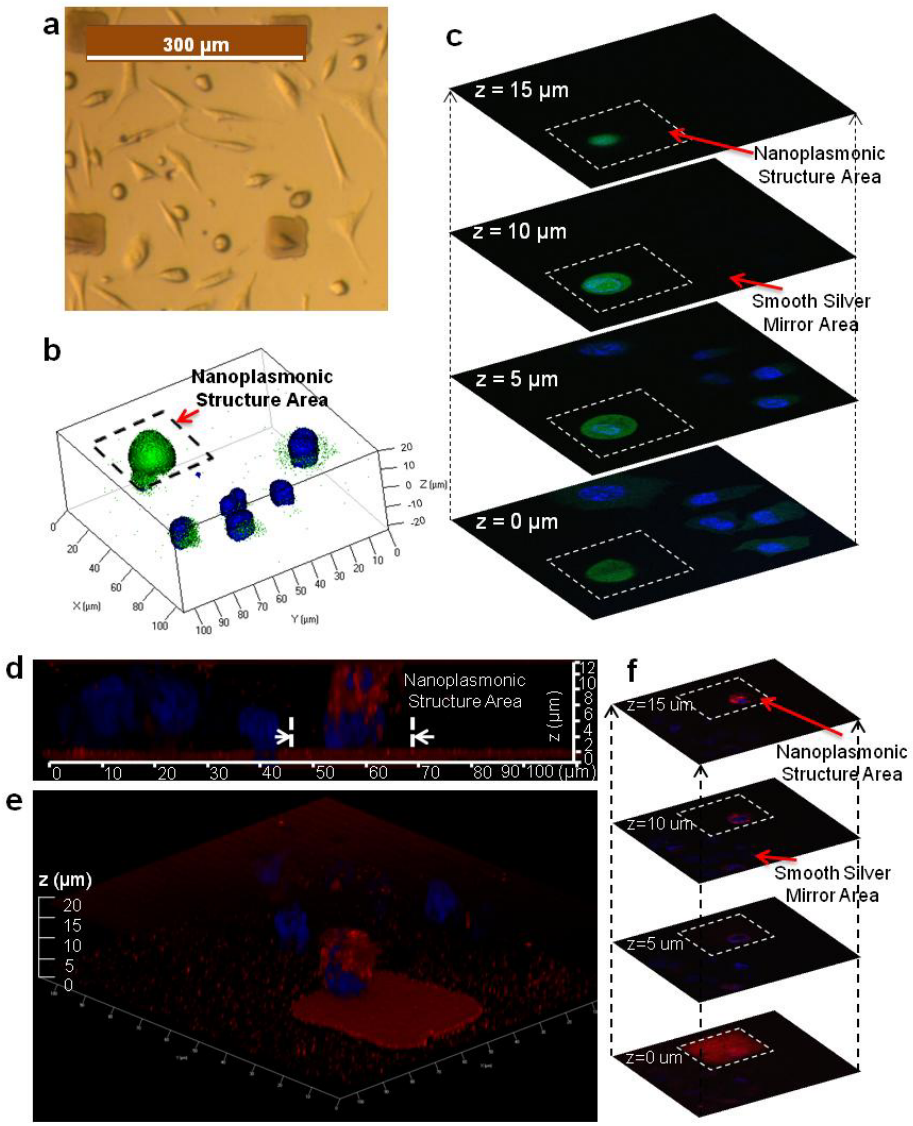

Figure 3. Living cell confocal fluorescence microscopy imaging assisted by nanoplasmon CORE method (a) Bright field image of large number of cells grown on the substrate (b) 3-D confocal image of Chinese Hamster Ovary (CHO) cells on the nanopillar plasmonic structure. (c) Vertical cross-section of the cells at different z-position. (d, e) Fluorescence enhancement away from the substrate. (f) The vertical cross-section (z-stack) image for the cell showing that the cell membrane fluorescence enhancement on the nanoplasmonic substrate is extending up to the top position on the spheroidal cell, around 15 μm above the nanoplasmonic substrate.

Downloaded From: http://proceedings.spiedigitallibrary.org/ on 04/22/2017 Terms of Use: http://spiedigitallibrary.org/ss/termsofuse.aspx

In Fig. 3(b) the fluorescence enhancement on cytoplasm (in green) is evident due to the fact that the cytoplasms of other cells on the smooth silver surfaces are hardly visible even though they are in the same imaging planes, although the nuclei are clearly observable for all cells. As shown in Fig. 3(c), z = 0 denotes on the surface of the substrate and z > 0 is away from the surface. The far field enhancement (at distance > 10 μm) for the fluorophore labeled to the cytoplasm of the CHO cell can be seen. The vertical cross-sectional cell images (Fig. 3c) at various z-positions show that the strong cytoplasm calcium fluorescence enhancement on the nanoplasmonic substrate is extending even up to the top position on the spheroidal cell, around 12 μm above the nanoplasmonic substrate and far beyond the 100 nm domain of metal surface enhanced fluorescence. However the fluorescence enhancement for the nucleus fluorescence is relatively modest due to the mismatch of excitation light and optical resonance wavelengths as well as the surface bounded WGM. For another set of experiment with cell membrane and nucleus labeled by red and blue emission fluorophores, the x-z plane cross-section image is shown (Fig. 3d). Due to overwhelmingly high fluorescence enhancement for the 3D cell membrane on the nanoplasmonic substrate, the other cell membrane on the smooth silver surface are not visible under such a high intensity contrast. However, fluorescence intensity of the cell nucleus on the nanopillar array substrate and that on the smooth silver surface are comparable, again confirming that the huge fluorescence enhancement is resulted from the nanoplasmon coupled WGM optical resonance and mainly occurs near the surface, not the center, of the cell membrane microcavity structure. To further prove the far field intracellular fluorescence enhancement is not due to the previously known metal enhanced fluorescence mechanism, we intentionally keep the fluorophore staining solution with the cells during this imaging experiment. From the x-z plane cross-sectional image (Fig.3d), one can see blue and red fluorescence, especially red fluorescence, from the fluorophore molecules are visible near the immediate substrate surface while not discernable at all above the substrate surface except in the cell sitting on nanoplasmonic structure. The far field fluorescence enhancement is further elucidated from the 3-D z-stack images of number of cells on smooth as well as nanopillar substrate (Fig.3f). Due to overwhelming fluorescence enhancement at far field, the fluorescent-labeled cell membrane can be seen only for the cell on the top of nanoplasmonic structure (Fig.3e). The vertical cross-sectional cell images (Fig. 3f) at various z-position again confirmed that the strong cell membrane fluorescence enhancement on the nanoplasmonic substrate is extending up to the top position on the spheroidal cell, around 15 μm above the nanoplasmonic substrate, which is far beyond the 100 nm domain of metal surface enhanced fluorescence.

4. QUANTITATIVE CELL IMAGING ANALYSIS

The quantitative analysis for fluorescence enhancement factor is performed by comparing the average fluorescence intensity at each depth (z-coordinate) of the z-stack images taken by confocal microscope. The average fluorescence intensities for the cell membrane, cytoplasm and nucleus are shown in Fig. 4. Here, increasing z denotes imaging plane away from the substrate surface i.e. z = 0 is on the substrate. The actual height or thickness of the cell is around 12 μm or z = 12 μm. On the cell membrane we observed a 23 fold fluorescence intensity increase on the nanoplasmonic substrate compared to that on the smooth silver mirror surface at the same imaging plane around z = 6 μm. Given that the smooth mirror surface can provide approximately 5 fold fluorescence enhancement which was confirmed from the fluorescence spectroscopy experiment (Fig. 6a), the total far field fluorescence enhancement factor for the cell membrane obtained by the Nanoplasmon CORE technology will be 115 folds with respect to a glass slide surface, which is much higher than the conventional metal enhanced fluorescence in near field, that is, approximately 40 folds with respect to a glass slide surface according to our measurement. Even by comparing the maximum fluorescence intensity measured on the smooth silver surface (at z = 0 μm) and that on the nanoplasmonic substrate (at z = 7 μm), there is still a 14 fold increase on the nanoplasmonic substrate with respect to the smooth silver surface. Most interestingly and worth noting, the maximum fluorescence enhancement on the silver coated nanopillar array structure is found at an imaging plane far away from the surface (z = 6~8 μm or mid-plane of the cell microcavity), which obviously cannot be explained by conventional metal enhanced fluorescence mechanisms. Figure 4a also shows that the silver nanocone structure (due to metal enhanced fluorescence) provides a 8 fold increase near the surface in the fluorescence intensity which is the nanostructure enhanced fluorescence measured for the nanoplasmonic structure and the maximum enhancement actually occurs at a plane away from the surface at z = 7 μm. The distance between two peaks is around 7 μm, which is approximately equals to the radius of the spheroidal CHO cell for the current configuration. The well-known fact that WGM optical resonance occurs near the equatorial plane of microcavity confirms the proposed Nanoplasmon CORE mechanism. Similar intensity enhancement is observed for fluorophores labeled to the cell cytoplasm on the nanopillar plasmonic structure as compared to the cells on the smooth silver surface (Fig. 4c). For the reason that the intracellular WGM optical resonance primarily resides near the cell membrane, the fluorescence enhancement becomes lower when fluorophore is labeled on cytoplasm calcium (approximately 70 folds with respect to the case on glass slide) as compared to when it is labeled to the cell membrane. As shown in Fig. 4b & 4d, the peak fluorescence intensity for the nucleus of the cell near the smooth

Downloaded From: http://proceedings.spiedigitallibrary.org/ on 04/22/2017 Terms of Use: http://spiedigitallibrary.org/ss/termsofuse.aspx

surface is slightly higher than that of the cell nucleus on the nanopillar structure. However, the fluorescence intensity of the fluorophore labeled to the nucleus on the nanopillar structure is higher than the cells on the smooth surface at far field. To illustrate our point more clearly, cells on two control samples (glass and smooth silicon substrate) and nanoplasmonic structure are imaged using the same imaging parameters set up (laser power of 1.8%, pixel dwell time of 2.55 μs). As shown in Fig. 4 e, f & g the higher fluorescence intensity for the cells on nanoplasmonic structure can be clearly seen. In fact with this higher power long integration time setting the cell image intensity on nanoplasmonic structure becomes saturated due to the extremely high enhancement.

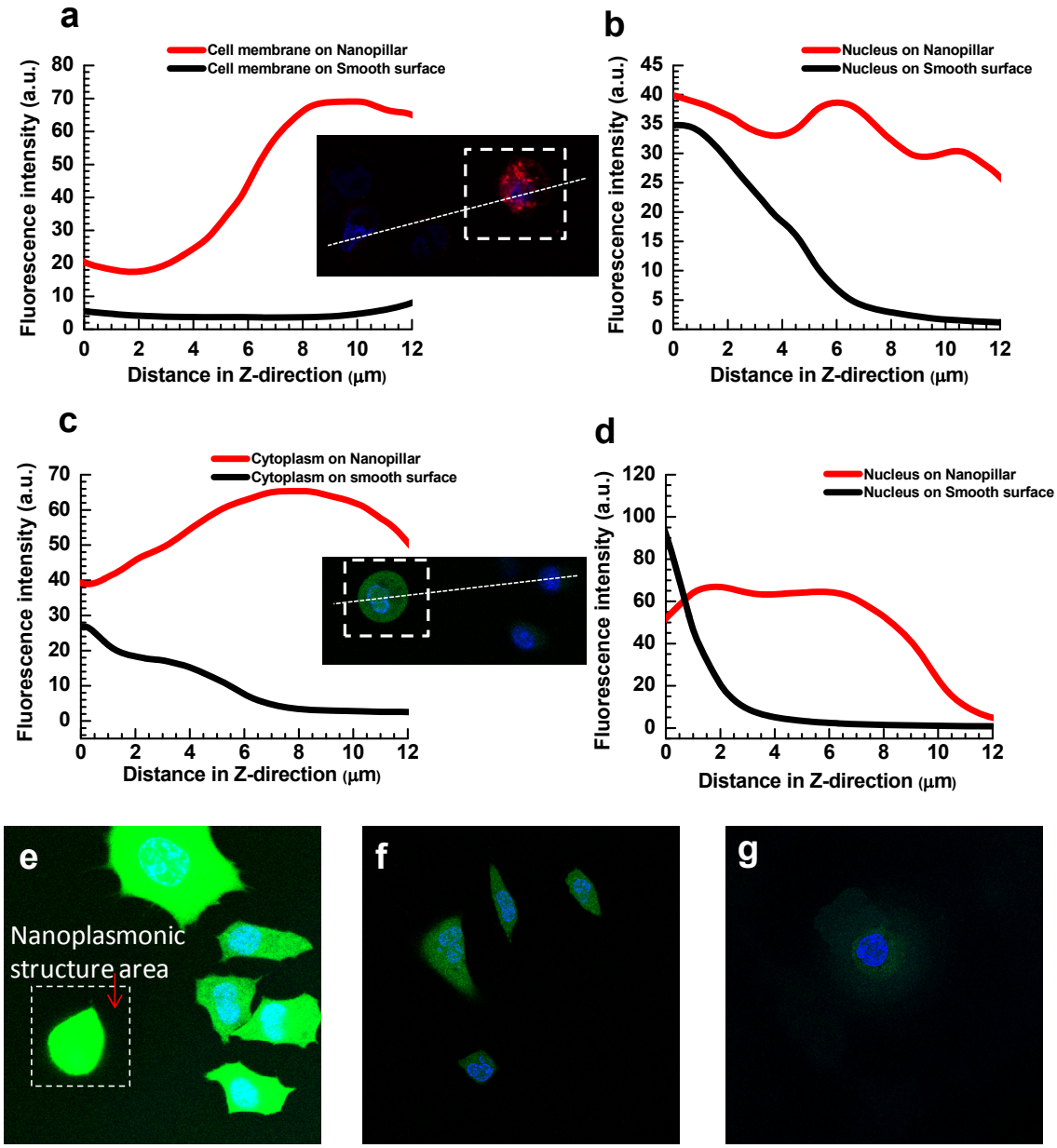

Figure 4. Quantitative analysis of fluorescence enhancement for (a-b) dye labeled to cell membrane and nucleus of CHO cell on the nanoplasmonic substrate; (c-d) for dye labeled to cell cytoplasm and nucleus of CHO cell on the nanoplasmonic substrate. Confocal cell imaging with identical laser power setting (0.48 mW) and pixel dwell time (2.55 us) for cells on (e) nanoplasmonic substrate (f) smooth silicon substrate and (g) glass substrate.

Downloaded From: http://proceedings.spiedigitallibrary.org/ on 04/22/2017 Terms of Use: http://spiedigitallibrary.org/ss/termsofuse.aspx

5. OPTICAL CHARACTERIZATION AND CONTROL EXPERIMENT

As a control experiment, the cells are imaged on a silicon nanopillar substrate (without silver coating layer). The fluorescence intensity of the cytoplasm on the silicon nanopillar and on the smooth silicon surface is quite similar (Fig. 5). This demonstrates the fact that special nanoplasmonic structure, not just dielectric nanostructure, is required for the coupled WGM optical resonance and the consequent enhanced fluorescence.

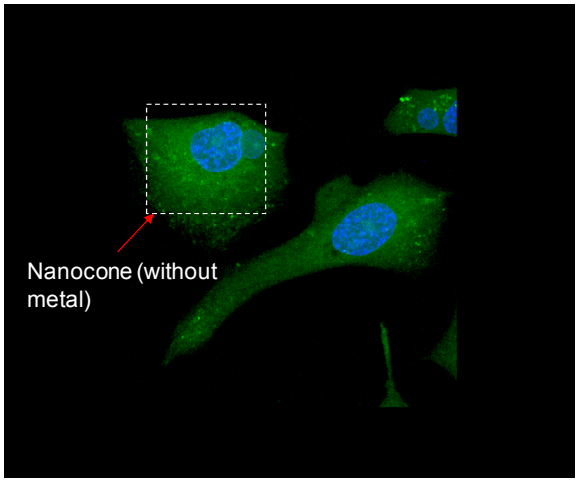

Figure 5. Confocal image of CHO cell on silicon nanocone control sample without any metal deposition.

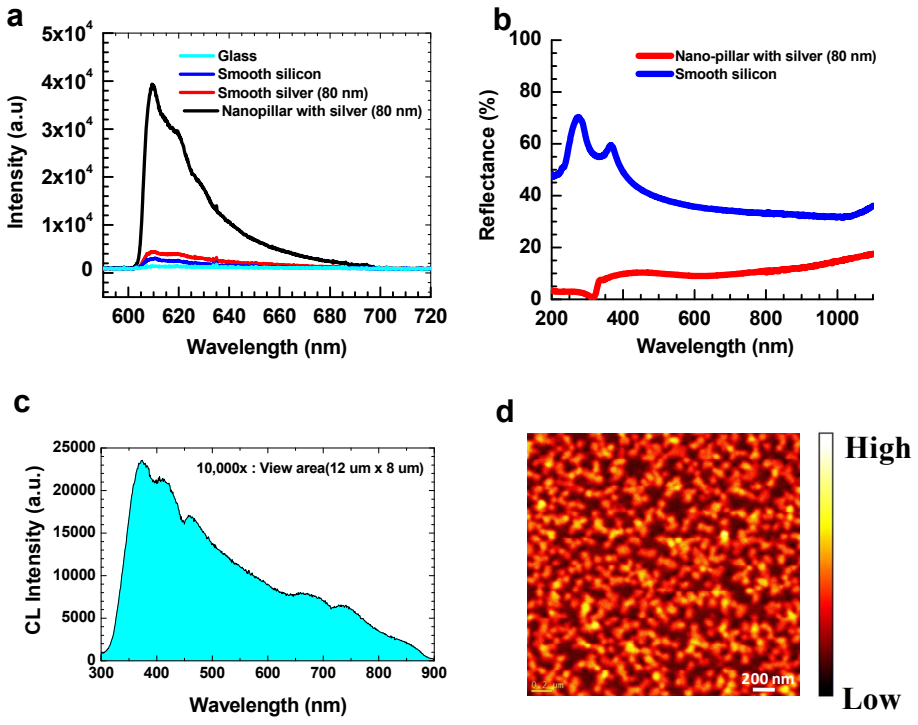

Figure 6. (a) Fluorescence spectroscopy experiment on the nanoplasmonic substrate. (b) Comparison of reflectance on smooth silicon substrate and nanoplasmonic substrate. (c-d) Cathodoluminescence (CL) spectra and panchromatic CL image of the nanoplasmonic substrate.

Downloaded From: http://proceedings.spiedigitallibrary.org/ on 04/22/2017 Terms of Use: http://spiedigitallibrary.org/ss/termsofuse.aspx

In order to discount the fluorescence enhancement at the far field due to a mirror reflection from the surface, the optical reflectance from the nanoplasmonic substrate is shown in Fig. 6b. The extremely low reflectance (< 10%) measured for the silver coated nanopillar structure in the visible range confirmed that most of the light incident on the nanoplasmonic substrate would be otherwise confined as plasmon polaritons within the surface near field if without the WGM coupling to optical resonance in spheroidal cell microcavity. Hence the enhanced fluorescence signal at far field cannot be justified by mirror reflection of the incident light. The cathodoluminescence (CL) experiment confirmed that the nanoplasmonic structure support multiple plasmon peaks (Fig. 6 c) and can provide high electromagnetic field as seen from the panchromatic CL image (Fig. 6 d).

We also compare the fluorescence lifetime of a fluorophore on the nanocone plasmonic structure with that on a smooth silver surface using fluorescence lifetime imaging microscopy (FLIM). As shown in Fig. 7(a) the lifetime of R6G gets quenched on the nanoplasmonic substrate. The comparison of modulus and phase component of the lifetime in Fig. 7(e) showed that the lifetime decay in free solution is a single component process whereas on nanoplasmonic substrate it follows a multi-component decay process. The fluorescence enhancement on the nanoplasmonic substrate is quite clear in Fig. 7(f). The lifetime of a fluorophore in free space is given by $\tau_0 = 1/(\Gamma + k_{NR})$ where Γ is the radiative decay rate and k_{NR} is the non-radiative decay rate. Similarly, the quantum yield of a dye in free space can be written as $Q_0 = \Gamma/(\Gamma + k_{NR})$. Further, in the presence of metal nanostructure, the quantum yield (Q_m) and lifetime (τ_m) of the fluorophore gets modified as $Q_m = (\Gamma + \Gamma_m)/(\Gamma + \Gamma_m + k_{NR,m})$ and $\tau_m = 1/(\Gamma + \Gamma_m + k_{NR,m})$ respectively.

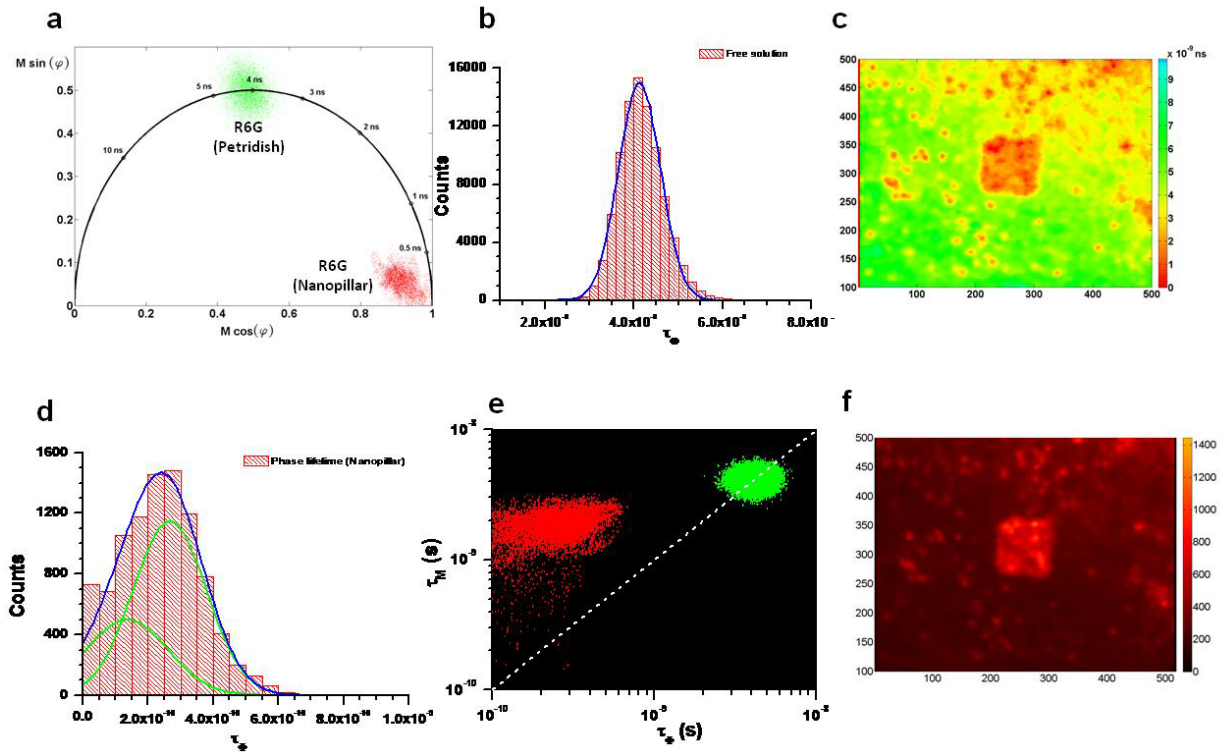

Figure 7. (a) Polar plot obtained from FLIM experiment. (b) Histogram showing intrinsic lifetime of R6G in free solution measured using FLIM. (c) Lifetime plot on the nanoplasmonic substrate. The square area is the nanoplasmonic region and the outside is the smooth silver region. (d) Lifetime of R6G measured on the nanocone area. (e) Comparison of phase and modulus lifetime on the nanoplasmonic substrate. (f) Fluorescence intensity enhancement on the nanoplasmonic area.

Downloaded From: http://proceedings.spiedigitallibrary.org/ on 04/22/2017 Terms of Use: http://spiedigitallibrary.org/ss/termsofuse.aspx

Hence, decrease in lifetime is an indication of increase in the total decay rates. Since, decrease in lifetime is also accompanied by increase in fluorescence intensity, there should be an increase in the radiative decay rates due to increase in total decay rates. As the fluorescence lifetime is the average time the fluorophore spend at the excited state, reduction in lifetime means fluorophore can undergo more number of cycles before photobleaching. Due to enhanced fluorescence on the nanoplasmonic substrate one can afford to use minimum laser power and pixel dwelling time, which further limits the chances of photobleaching. Finally, the decreased lifetime and enhanced radiative decay rate of the fluorophore on the nanocone plasmonic structure will contribute to better photo stability of the fluorophore and enhanced quantum yield in visible wavelength range.

6. MECHANISM OF ENHANCEMENT

The whispering-gallery modes are generally described by Maxwell vector wave equation, which reduces to Helmholtz equation for a homogeneous material with azimuthal symmetry [17] as $\nabla^2\psi_{l,m,n}(r,\theta,\phi)+k^2\psi_{l,m,n}(r,\theta,\phi)=0$ where $k=k_0(\varepsilon\mu)^{1/2}$ and $k_0=\omega/c$. The field can be found using the separation of variable technique as $\psi_{l,m,n}(r,\theta,\phi)=N_s\psi_r(r)\psi_\theta(\theta)\psi_\phi(\phi)$ where r,θ and ϕ describe the radial, polar and azimuthal direction of field respectively and N_s is the normalizing coefficient derived in reference [18]. Whispering gallery modes are characterized by three mode numbers (n,m,l) which are the radial, azimuthal (or equatorial) and angular (or polar) mode numbers, respectively. The radial part of a sphere WGM can be described by spherical Bessel functions with an external evanescent tail, while the polar (longitudinal) field dependence follows spherical harmonics, and the equatorial (azimuthal or latitudinal) field variation is sinusoidal [18]. Finally, the integration strength between two interacting modes can be described by using coupled mode theory with writing the overlap integral. For example, the coupling between fibre mode and a perfect dielectric sphere can be written as [18]

$$\kappa=\frac{k^2}{2\beta_f}\int_x\int_y\left(n_s^2-n_0^2\right)F_0\,\psi_{l,m,n}\,dx\,dy$$

where n_s, n_0 are the refractive index of sphere and surrounding medium respectively. Here, F_0 describes the field of an optical fibre, the analytical solution for which is well known [18]. Similarly, for the coupling between surface plasmon mode and WGM, we have to find an expression similar to F_0 in order to write the overlap integral, which generally describe the rate of increase in amplitude of the sphere mode (and hence for fibre coupled WGM, κ^2 is the amount of power coupled out of the fibre into the sphere per revolution) [11]. Now in order to describe the coupling mode between surface plasmon (SP) and dielectric WGM can be written by replacing F_0 in the overlapping integral by the expression $F_0=N_{sp}\exp(-z/\Delta z_D)$ *if* $z>0$ and $F_0=N_{sp}\exp(-z/\Delta z_M)$ *if* $z<0$. It should also be noted that the surface plasmon field in the metal also decays exponentially with increasing distance from the interface and the penetration depth is given by $\Delta z_M=\Delta z_D n_D^2/(-\varepsilon_M')$. Here the subscript D is used for dielectric and M is used for metal.

7. EXPERIMENT WITH TRANSFECTED CANCER CELLS

Transfection is like tagging applications, which utilize certain protein as a reporter protein for monitoring of gene expression and protein localization on a real-time basis after insertion of signal sequences into the gene. The typical imaging window post transfection is about 36-54 hrs. The limitation is imposed because of low fluorescence intensity at early stage of transfection. Due to significant fluorescence enhancement on nanoplasmonic substrate, we can possibly image the early stage of transfection. In the present experiment, we transfected a cervical cancer line (HeLa) with a fluorescent protein (mCherry-paxillin) and grew them on nanoplasmonic as well as traditional petridish (glass substrate). The cells were analyzed by confocal microscopy 12-18 hr post transfection. Figure 8(a) shows the confocal fluorescence image of transfected cells on petridish. As expected, the cells did not show any contrast for the target protein paxillin.

Downloaded From: http://proceedings.spiedigitallibrary.org/ on 04/22/2017 Terms of Use: http://spiedigitallibrary.org/ss/termsofuse.aspx

However, the cells on the nanoplasmonic substrate clearly showed the paxillin locations (Fig. 8(b)). Further, we observed enhanced fluorescence for cells on the nanoplasmonic substrate.

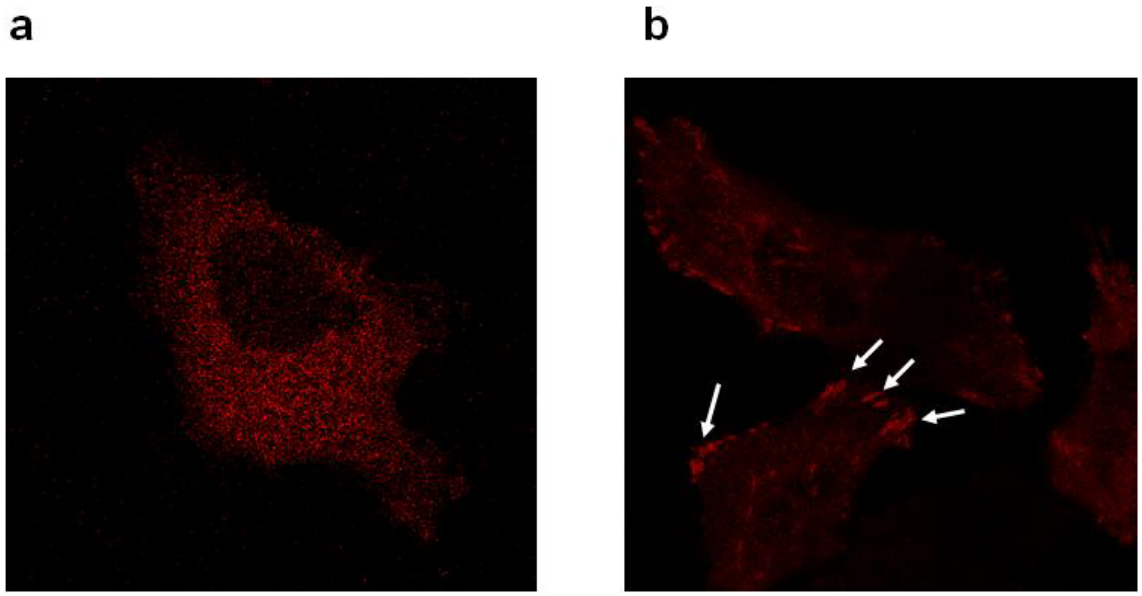

Figure 8. Confocal fluorescence image of HeLa cell transfected with mCherry-paxillin. (a) Cells on petridish (b) Cells on nanoplasmonic substrate.

8. CONCLUSION

We demonstrated that the nanoplasmon CORE technology can enable significantly enhanced 3D fluorescence cell imaging capability with unprecedented high sensitivity and photo stability. We have showed that the nanoplasmon surface can enhance the fluorescence signal from a cell membrane (FM 1-43 FX) by 115 folds and from a cell cytoplasm (Fluo-4, AM) by 70 folds. We anticipate that the nanoplasmonic surface could be less phototoxicity on the cells and less photobleaching on the dye (allowing longer time-lapse acquisition) and hence will be an ideal candidate as microscopy substrates. We envision the immediate impact of this new technology in all cell biology especially membrane protein studies to facilitate new fundamental discoveries and better clinical diagnostics. The nanoplasmon CORE device can be used in a confocal fluorescence microscopy system just like using a glass slide or petri dish to support cell samples. Hence by using this new technology, molecular cell biologists can immediately enjoy a 2-3 orders of magnitude higher 3D fluorescence cell imaging sensitivity without additional modifications to the current confocal microscopy instrumentation or procedure. More importantly, the presented novel biotechnology offers the opportunity to capture single molecular events in living cells, observe very early stage protein expressions after genetic transfection, and discover new basic mechanisms in cytoskeletal dynamics, cell adhesion and cell migration as well as membrane trafficking.

REFERENCES

[1] Lichtman, J.W. and Conchello, J. A., “Fluorescence microscopy”, Nature Methods 2 (12), 910-919 (2005).
[2] Moal, E.L., Fort, E, Fort, S.L., Murata, A.J.H., Cordelieres F.P. & Fontaine-Aupart, M.P., “Mirror slides for high-sensitivity cell and tissue fluorescence imaging”, Journal of Biomedical Optics 12(2), 024030 (2007).

Downloaded From: http://proceedings.spiedigitallibrary.org/ on 04/22/2017 Terms of Use: http://spiedigitallibrary.org/ss/termsofuse.aspx

[3] Moal, E.L., Fort, E, Fort, S.L., Cordelieres F.P., Fontaine-Aupart, M.P. & Ricolleau, C., "Enhanced Fluorescence Cell Imaging with Metal-Coated Slides", Biophysical Journal, 92, 2150-2161 (2007).
[4] Zhang, J., Fu, Y., Liang, D., Zhao, R.Y. and Lakowicz, J.R., "Enhanced Fluorescence Images for Labeled Cells on Silver Island Films", Langmuir, 24, 12452-12457 (2008).
[5] Aslan, K. et al., "Metal-enhanced fluorescence: an emerging tool in biotechnology", Current Opinion in Biotechnology, 16, 55-62 (2005).
[6] Hwang, E., Smolyaninov, I.I. and Davis, C.C., "Surface Plasmon Polariton Enhanced Fluorescence from Quantum Dots on Nanostructured Metal Surfaces", Nano Lett. 10, 813–820 (2010).
[7] Ray, K., Szmacinski, H., Enderlein, J and Lakowicz, J.R., "Distance dependence of surface plasmon-coupled emission observed using Langmuir-Blodgett films", Applied Physics Letters, 90, 251116 (2007).
[8] Rosenblatt, D., Sharon, A. and Friesem, A. A., "Resonant grating waveguide structures", IEEE Journal of Quantum Electronics, 33, 11, 2038-2059 (1997).
[9] Arnold, S., "Microspheres, Photonic Atoms and the Physics of Nothing", American Scientist, 89, 414-421 (2001).
[10] Vollmer, F. and Arnold, S., "Whispering-gallery-mode biosensing: label-free detection down to single molecules", Nature Methods, 5 (7), 591-596 (2008).
[11] Barnes, W.L., Dereux, A. and Ebbesen, T.W., "Surface plasmon subwavelength optics", Nature, 424, 824-830 (2003).
[12] Min, B. et al., "High-Q surface-plasmon-polariton whispering-gallery microcavity", Nature, 457, 455-459 (2009).
[13] Hon, N.K. and Poon, A.W., "Surface plasmon resonance-assisted coupling to whispering-gallery modes in micropillar resonators", J. Opt. Soc. Am. B, 24 (8), 1981-1986 (2007).
[14] Stockman, M.I., "Nanofocusing of Optical Energy in Tapered PlasmonicWaveguides", Physical Review Letters, 93, 137404 (2004).
[15] Sheeley D.M., Merrill B.M. and Taylor L.C., "Characterization of Monoclonal Antibody Glycosylation: Comparison of Expression Systems and Identification of Terminal α-Linked Galactose", Anal. Biochem. 247, 102-110 (1997).
[16] Werner, R.G, Noe, W., Kopp, K. and Schluter M. Arzneimittel-Forschung, 48(8), 870–880 (1998).
[17] Oraevsky, A.N., "Whispering-gallery waves", Quantum Electronics, 32 (5), 377 (2002).
[18] Little, B.E., Laine, J.P. and Haus, H.A., "Analytic Theory of Coupling from Tapered Fibers and Half-Blocks into Microsphere Resonators", J. Lightwave Tech., 17, 704 (1999).

Downloaded From: http://proceedings.spiedigitallibrary.org/ on 04/22/2017 Terms of Use: http://spiedigitallibrary.org/ss/termsofuse.aspx